GEOGRAPHY
Jurnal Kajian, Penelitian dan Pengembangan Pendidikan
http://journal.ummat.ac.id/index.php/geography
Vol. 14, No. 2, September 2026, Hal. 327-343
e-ISSN 2614-5529 | p-ISSN 2339-2835

ANALYSIS OF FLOOD INUNDATION DISTRIBUTION BASED ON METEOROLOGICAL FACTORS AND LAND COVER USING HEC-RAS IN THE TUKAD BADUNG WATERSHED (CASE STUDY: THE BALI FLOODS OF SEPTEMBER 9–10, 2025)

Naufal Ilham Habibi[1]*, Ania Maulidiah Nisa[2]

[1,2]Climatology Department, Indonesia of Meteorology Climatology and Geophysics (STMKG), Tangerang, Indonesia,
naufalhabibi542@gmail.com, aniamaulidiahnisa@gmail.com

ABSTRACT

Abstract: The September 9–10, 2025, flood in the Tukad Badung Watershed was the most severe event of the past decade, triggered by extreme rainfall that resulted in 16 fatalities and widespread inundation across several regencies and cities in Bali. This study aims to analyze meteorological conditions and land cover during the flood event and to model flood inundation using HEC-RAS software. Data used include meteorological parameters (rainfall, temperature, air pressure, wind speed and direction, and evapotranspiration) and land cover (land use land cover and soil type). Results indicate abnormal meteorological conditions at both observation stations: ARG Abiansemal recorded rainfall of 284.6 mm, temperature of 22.72°C, pressure of 1,004.34 hPa, wind speed of 3.3 m/s, wind direction from the northwest, and evapotranspiration of 0.171–0.172 mm/h; while AWS Tuban recorded rainfall of 116 mm, temperature of 23.59°C, pressure of 993.23 hPa, wind speed of 4.48 m/s, wind direction from the northwest, and evapotranspiration of 0.120–0.121 mm/h. built up area-dominated land cover and clay loam soils from upstream to downstream further intensified the flooding. HEC-RAS simulations produced inundation depths of 1–3 meters, accurately representing actual flood conditions with a hit rate of 83.33%.

Keyword: *Flood; Meteorology; Land Cover; HEC-RAS; Tukad Badung Watershed*

Abstrak: Banjir yang terjadi pada 9–10 September 2025 di Daerah Aliran Sungai (DAS) Tukad Badung merupakan peristiwa terparah dalam satu dekade terakhir, yang dipicu oleh curah hujan ekstrem yang mengakibatkan 16 korban jiwa dan genangan luas di beberapa kabupaten dan kota di Bali. Penelitian ini bertujuan untuk menganalisis kondisi meteorologi dan tutupan lahan selama peristiwa banjir tersebut serta memodelkan genangan banjir menggunakan perangkat lunak HEC-RAS. Data yang digunakan meliputi parameter meteorologi (curah hujan, suhu, tekanan udara, kecepatan dan arah angin, serta evapotranspirasi) dan tutupan lahan (penggunaan lahan, tutupan lahan, dan jenis tanah). Hasil penelitian menunjukkan kondisi meteorologi yang tidak normal di kedua stasiun pengamatan: ARG Abiansemal mencatat curah hujan sebesar 284,6 mm, suhu 22,72°C, tekanan 1.004,34 hPa, kecepatan angin 3,3 m/s, arah angin dari barat laut, dan evapotranspirasi sebesar 0,171–0,172 mm/jam; sedangkan AWS Tuban mencatat curah hujan sebesar 116 mm, suhu 23,59°C, tekanan 993,23 hPa, kecepatan angin 4,48 m/s, arah angin dari barat laut, dan evapotranspirasi sebesar 0,120–0,121 mm/jam. Tutupan lahan yang didominasi kawasan permukiman dan tanah lempung liat dari hulu ke hilir semakin memperparah banjir. Simulasi HEC-RAS menghasilkan kedalaman genangan 1–3 meter, yang secara akurat menggambarkan kondisi banjir sebenarnya dengan tingkat akurasi sebesar 83,33%.

Kata kunci: *Banjir; Meteorologi; Tutupan Lahan; HEC-RAS; Daerah Aliran Sungai Tukad Badung*

Article History:
Received: 28-07-2026
Revised : 06-08-2026
Accepted: 17-08-2026
Online : 04-09-2026

A. INTRODUCTION

Floods are one of the most frequent hydrometeorological disasters and pose a threat to human life in Indonesia (Sarifah et al., 2024; Sulistya, 2022). National Disaster Management Agency (BNPB) (2025) recorded 1,420 flood incidents in 2024. These incidents affected 6,301,056 people and forced roughly 77.44% of them to evacuate their homes. The disasters also caused substantial economic losses and environmental damage (Bakar, 2024). Flooding occurs when water volume exceeds an area's capacity and overflows into surrounding land (Asdak, 2010; Desalegn & Mulu, 2021). This phenomenon does not stem from a single cause but is triggered by two interrelated main factors: natural factors and human factors (Danumah et al., 2016). From a natural perspective, Climate change intensifies extreme rainfall events and disrupts seasonal predictability, making flood mitigation increasingly difficult (Ahmad & Afzal, 2022; Danumah et al., 2016). Meanwhile, from a human perspective, the rapid pace of urbanization, land-use conversion, and uncontrolled development expansion are gradually eroding the soil's ability to absorb rainfall. As a result, surface runoff increases drastically and the risk of flooding grows (Peker et al., 2024; Selçuk et al., 2016). These two factors converge most critically in river basins.

A Watershed (DAS) is a land area encompassing a river and its tributaries, topographically bounded by mountain ridges and hills, which serves to collect, store, and convey rainwater to the sea via the main river (Asdak, 2010). Changes in watershed condition directly affect its function as a flow regulator (Jabbar et al., 2023). The Tukad Badung Watershed, which plays a vital role in the lives of the Balinese people, has experienced such conditions (Wiarta et al., 2008). Population growth, land-use conversion, river siltation, and the inappropriate use of public spaces have reduced the watershed's capacity to store water, leading to annual flooding during the rainy season (Aryastana, 2015). Under extreme rainfall conditions the watershed can also flood outside the rainy season. Research by Aulia et al. (2023) indicates that under specific conditions resulting from extreme rainfall, flooding in the Tukad Badung Watershed can occur between June and September. This finding aligns with the flood event on September 9–10, 2025. The BBC (2025) reported this as the worst flood in the past decade. It struck the districts of Jembrana, Gianyar, Tabanan, Klungkung, and the city of Denpasar and killed 16 people. The flood disaster was caused by extreme rainfall that relentlessly pounded the region (BBMKG Wilayah III, 2025). According to Balipost (2025), the flood peaked on September 10, 2025, at 5:00 a.m. WITA, with water levels reaching 3 meters.

Therefore, an analysis of the flood's distribution is therefore necessary to determine its severity.

The Hydrologic Engineering Center's River Analysis System (HEC-RAS), developed by the U.S. Army Corps of Engineers (USACE), is used to model flood inundation and analyze complex hydraulic problems (Bragg et al., 2025; Wijayanto & Helda, 2022). The HEC-RAS software can simulate both steady-state and unsteady-state river flow in both one and two dimensional (Iswardoyo & Satria, 2023). It can also display surface runoff from rainfall simulations and represent water uptake through CN or Green Ampt infiltration (Bragg et al., 2025). The data used in the modeling include Digital Elevation Model (DEM) maps, longitudinal and cross-sectional data, boundary conditions, Manning's coefficient for flood discharge, and rainfall data (Suryadi et al., 2022).

Several studies have applied HEC-RAS in Bali. A study by Wiarta et al. (2008) on the Tukad Badung River found that even at a 50-year recurrence interval, the river was still capable of accommodating flood discharge. The groundwater table remained below the elevation of the left bank and the river. A related study by Suryatmaja et al. (2024) used HEC-RAS to model drainage capacity. The results indicated that drainage capacity was sufficient for the 800–1,000-meter segment, while the 0–800-meter segment no longer met the requirements. Both studies focused only on channel capacity rather than on flood inundation patterns tied to meteorological conditions and land cover during an actual event. Therefore, this study aims to identify and analyze the meteorological conditions and land cover present when the September 9–10 flood disaster occurred. It also aims to analyze flood inundation patterns verified against actual flood occurrence points. The research is expected to inform the public about the factors causing the disaster and to support mitigation recommendations from relevant agencies should similar conditions recur.

B. METHOD

1. Study Area

This study was conducted in the Tukad Badung watershed, Bali Province. The watershed lies between 08°25'31" and 08°44'49" South Latitude and between 115°10'23" and 115°16'27" East Longitude, covering Badung Regency and the City of Denpasar. It has an area of approximately 37.7 km^2 and a river length of 25.17 km (Wiarta et al., 2008). The watershed boundary in this study was obtained through delineation using the Hydrological Engineering Center Hydrologic Modeling System (HEC-HMS) as shown in Figure 1.

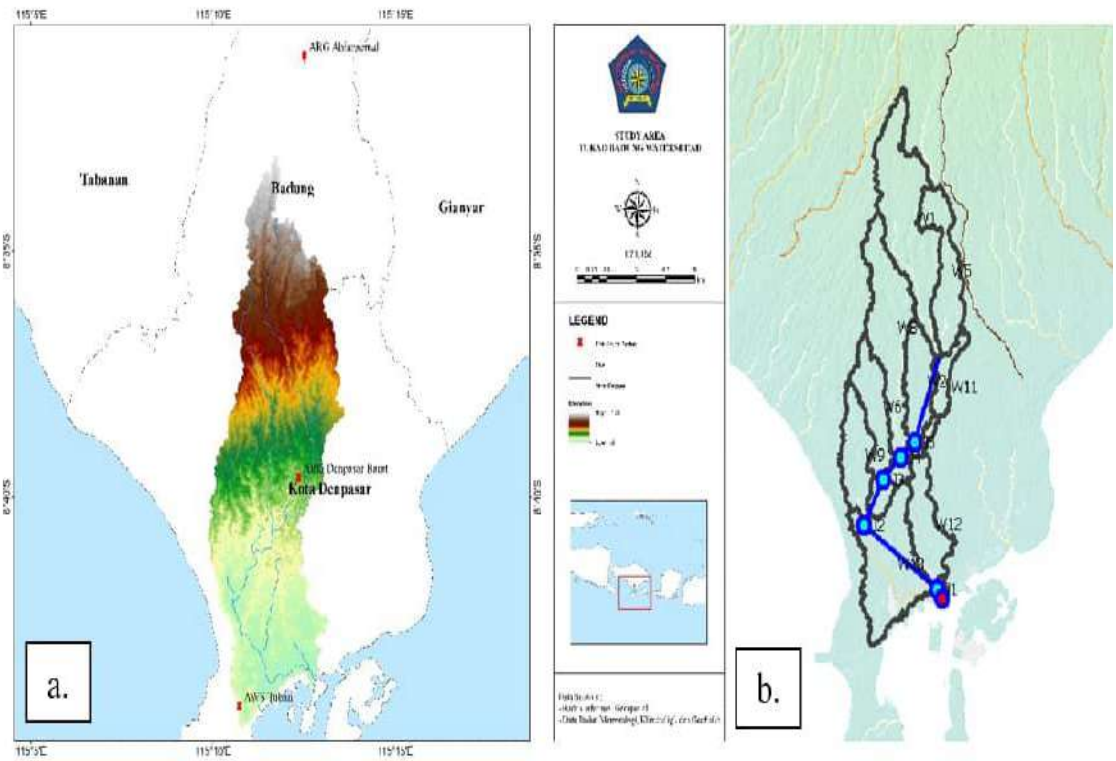

Figure 1. (a) Research Location, (b) Results of Watershed Delineation Using HEC-HMS

2. Dataset

Several datasets were used to analyze the causes and distribution of the flood. Meteorological data were used to examine flood causes from the perspective of atmospheric dynamics (Setiawan et al., 2022). This included rainfall data from BMKG's automatic rain gauges at ARG Abiansemal and Denpasar Barat and the AWS in Tuban, along with ERA5 reanalysis data on surface air pressure, 10 m wind u and v components, 2 m air temperature, surface net solar radiation, and surface net thermal radiation, the last three used to calculate potential evapotranspiration (Singer et al., 2021). These data also served as inputs for the HEC-RAS software at the BMKG rainfall gauge coordinates. Land cover and land use data were further used to analyze the physical surface factors of the Tukad Badung watershed contributing to the disaster. Details of all data used in this study are presented in Table 1.

Table 1. Dataset

No	Name	Spatial Resolution	Temporal Resolution	Unit	Source
1.	Digital Elevation Model (DEM) SRTM	30 m	2014	m	https://earthexplorer.usgs.gov/
2.	Rainfall data	-	Hourly from September 4–13, 2025	mm	https://awscenter.bmkg.go.id/base
3.	Surface pressure	$0.1^{\circ} \times 0.1^{\circ}$		Pa	
4.	10m u-component of wind			m/s	

5.	10m v-component of wind (m/s)		Hourly from September 4–13, 2025	m/s	https://cds.climate.copernicus.eu/
6.	Dew point temperature			K	
7.	2 m air temperature			K	
8.	Surface net solar radiation			J/m²	
9.	Surface net thermal radiation			J/m²	
10.	Land cover from sentinel-2	10 m/pixel	2024	m/pixel	https://livingatlas.arcgis.com/
11.	Soil type	250 m/pixel	2017	m/pixel	https://data.isric.org/
12.	Flood-affected areas	-	September 9–10, 2025 (12 events)	Events	https://dibi.bnpb.go.id/

3. Research Tools

A combination of software and analytical tools was used throughout the research process. Microsoft Excel was used to calculate and analyze rainfall data, while Google Colab was used to compute hourly potential evapotranspiration and each parameter's value at the BMKG rainfall gauge coordinates mentioned earlier. HEC-HMS was used to delineate the Tukad Badung watershed based on DEM data, and the resulting boundary served as the base terrain in HEC-RAS to analyze flood distribution during the September 9 to 10, 2025 flood event. QGIS was then used to map the results and verify the HEC-RAS model against actual flood locations.

4. Research Methods

The study consisted of several stages, including the following:

a. Collecting all data,
b. Delineating the watershed using HEC-HMS,
c. Calculating potential evapotranspiration using ERA5 data. Potential evapotranspiration represents the amount of water the atmosphere requires to calculate actual evapotranspiration, assuming unlimited water availability (Singer et al., 2021). In this study, hourly potential evapotranspiration is calculated and referred to as hPET, described by the following equation.

$$hPET_{x,t} = \frac{0.408\Delta(R_n - G) + \gamma(\frac{37}{T_a+273})u_2(e_s - e_a)}{\Delta + \gamma(1+0.34u_2)}$$

Where

R_n = hourly net radiation (MJ m^{-2}),
G = the soil heat flux (MJ m^{-2}),
γ = the psychrometric constant (kPa °C^{-1})
Δ = slope of saturation vapour pressure curve (kPa °C^{-1}),
T_a = hourly air temperature (°C) after converting from ERA5-Land temperature in K,
e_s = hourly saturation vapour pressure (kPa),
e_a = actual hourly vapour pressure (kPa),
u_2 = the hourly wind speed (m s^{-1}) at 2 m above the land surface

d. Extracting ERA5 values and potential evapotranspiration from grid points to the coordinates of BMKG rainfall gauges using the nearest neighbor approach, which yields better results than bilinear interpolation from the four surrounding grid cells (Lavers et al., 2022; Patra et al., 2025).
e. Calculating the Curve Number (CN) using Land Use Land Cover (LULC) and soil type data. The Curve Number estimates surface runoff, with higher values indicating greater runoff (Davie, 2019; Scharffenberg & Fleming, 2006). The determination of CN refers to the classification published by the United States Geological Survey (USGS).
f. Analyzing the flood inundation pattern by entering all data into HEC-RAS software. The inundation pattern is determined using the diffusion wave equation formulated by Brunner (2016) as follows.

$$\frac{\partial H}{\partial t} - \nabla.(\beta \nabla H) + q = 0$$

Where
H = water level (m),
t = time (s),
∇H = water level gradient
β = hydraulic diffusion coefficient (m^2 s^{-1}),
q = water inflow/outflow (m s^{-1}).

g. Validating the output against recorded flood event data using the Hit Rate (HR) method, also known as recall. In the context of flood mapping, recall indicates the proportion of actually flooded pixels that the model successfully detects. A higher recall means fewer flooded areas are missed, while a lower recall means the model misses more of the actually flooded areas (Shi et al., 2025; Swaminathan & Tantri, 2024). The formula used is as follows.

$$HR = \frac{TP}{TP + FN} \times 100\%$$

In the context of flood mapping, True Positive (TP) is a pixel correctly predicted as flooded that is indeed flooded in the reference data, while False Negative (FN) is a pixel that is actually flooded but fails to be detected by the model. A higher number of FNs means more flooded areas go undetected, resulting in an incomplete picture of actual flood conditions on the ground. The overall workflow of this research is shown in the following flowchart.

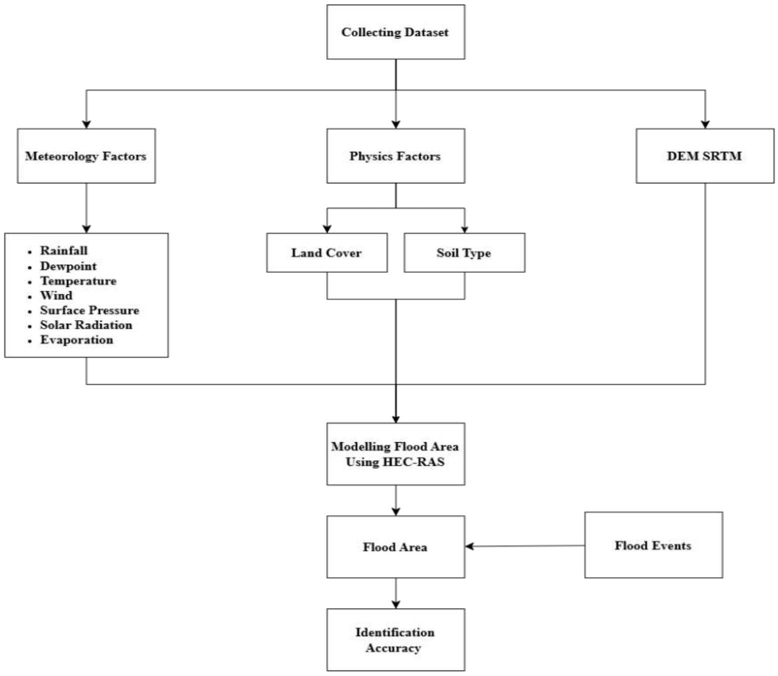

Figure 2. Flowchart Diagram

C. RESULTS AND DISCUSSION

1. Analysis Factor of Meteorology

Observations from two Automatic Rain Gauges (ARG) operated by the BMKG indicate significant rainfall variability during the period of September 4–13, as shown in Figure 3.

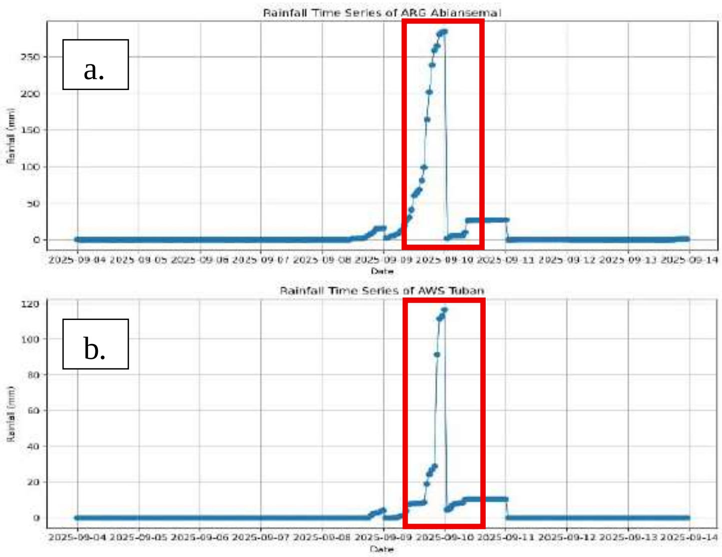

Figure 3. Time Series of Rainfall in (a) ARG Abiansemal and (b) AWS Tuban

Both stations showed similar temporal patterns, with rainfall beginning in the Tukad Badung area on September 9, 2025 and increasing in intensity until it peaked over the following days. The Abiansemal ARG, located in the upper watershed, recorded a total rainfall of 284.6 mm, while the Tuban AWS downstream recorded 116 mm during the same period. According to the Indonesian Meteorological, Climatological, and Geophysical Agency or BMKG (2023), rainfall at the Abiansemal ARG falls into the extreme category with an intensity exceeding 150 mm/day, while the Tuban AWS falls into the very heavy category at 100 to 150 mm/day. Such intensity over a short duration increases flood risk, particularly in urban areas, as the resulting river flow can exceed the streams' capacity to contain it (Wasko et al., 2021). This condition is supported by other meteorological factors including temperature, air pressure, wind speed, and wind direction, which depict conditions different from normal, as shown in Figures 4 and 5 below.

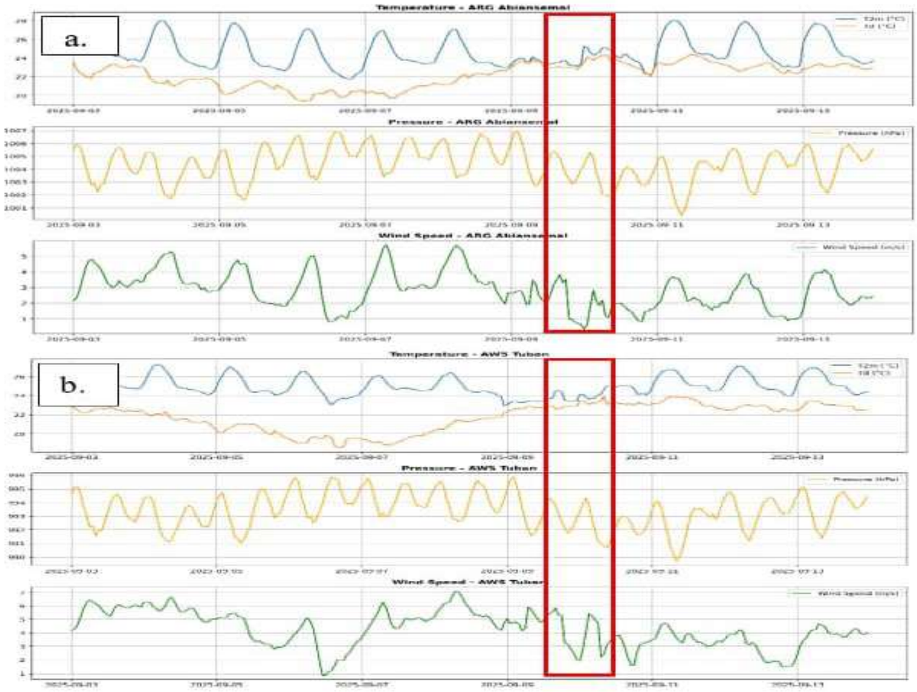

Figure 4. Time Series of Temperature, Pressure, Wind Speed in (a) ARG Abiansemal and (b) AWS Tuban

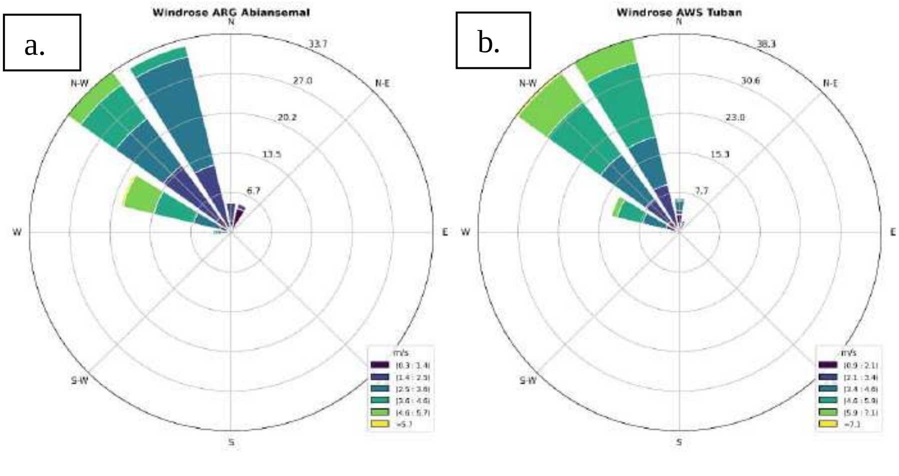

Figure 5. Windrose of Wind Direction in (a) ARG Abiansemal and (b) AWS Tuban

Based on Figure 4, an abnormal temperature change occurred on September 9, 2025 at ARG Abiansemal, with a smaller diurnal difference than on the days before or after the flood. The average temperature at that time was 22.72°C, while the dew point temperature showed a similarly small difference from the recorded temperature. This indicates high air humidity, which encouraged condensation and thereby increased cloud formation that blocked incoming solar radiation (Audah et al., 2017).

Air pressure readings showed relatively small diurnal variations compared to the days before or after the flood, averaging 1004.34 hPa. Such low pressure indicates surface warming, which triggers cloud formation by blocking incoming and outgoing radiation from the Earth's surface (Anggreni et al., 2018; Seto, 2011). This was reinforced by lower wind speeds averaging 3.3 m/s, as reduced wind speed also contributes to cloud formation and increased rainfall (Mulyana, 2014). A similar pattern occurred downstream at the Tuban AWS, which recorded an average air temperature of 23.59°C and dew point temperature of 22.77°C, alongside a decrease in air pressure to 993.23 hPa and wind speed to 4.48 m/s. Wind direction in both the upstream and downstream regions of the Tukad Badung watershed predominantly originated from the northwest, as shown in Figure 5. This pattern aligns with the westward-moving equatorial Rossby wave, which pushes moist air into the Bali region and enhances convective cloud growth along the Tukad Badung River Basin.

Evapotranspiration, which includes evaporation from water bodies and transpiration from vegetation, plays an important role in the hydrological cycle by determining the amount of water lost to the atmosphere through condensation, contributing to cloud formation and increasing the rainfall intensity that triggers flooding (Erwanto et al., 2021; Zhang & Wang, 2021). The evapotranspiration rate during the flood event on September 9, 2025 is presented in Figure 6 below.

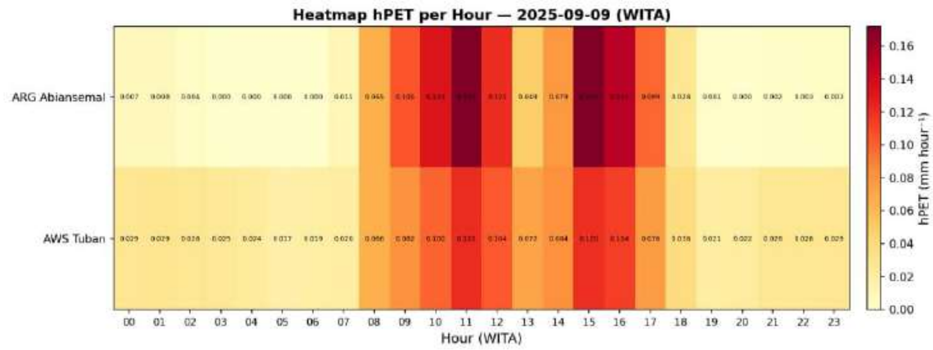

Figure 6. Heatmap Potential Evapotranspiration in ARG Abiansemal and AWS Tuban on September

Figure 6 shows that potential evapotranspiration peaks during daylight hours, consistent with Singer et al. (2021). At ARG Abiansemal, evapotranspiration peaked at 11:00 a.m. and 3:00 p.m. WITA, with values of 0.171 and 0.172 mm/hour respectively, while AWS Tuban recorded peaks at the same times of 0.121 and 0.120 mm/h. The consistently higher hPET at ARG Abiansemal is likely influenced by differences in land cover and elevation between the two locations. This diurnal pattern follows the daily cycle of shortwave radiation, which peaks in intensity during the day and increases the energy available for evaporation and transpiration. The resulting rise in atmospheric water vapor serves as raw material for cloud formation through condensation, increasing the likelihood of convective rain from afternoon into evening, a pattern commonly observed in tropical regions such as Bali (Qian, 2008).

2. Analysis Factor of Land Cover

In this study, LULC and soil type data were used to analyze the September 9 to 10, 2025 flood in Bali from the perspective of physical land surface characteristics, and to calculate the CN value used for estimating surface runoff from rainfall. The LULC, soil type, and CN are mapped respectively in Figure 7 below.

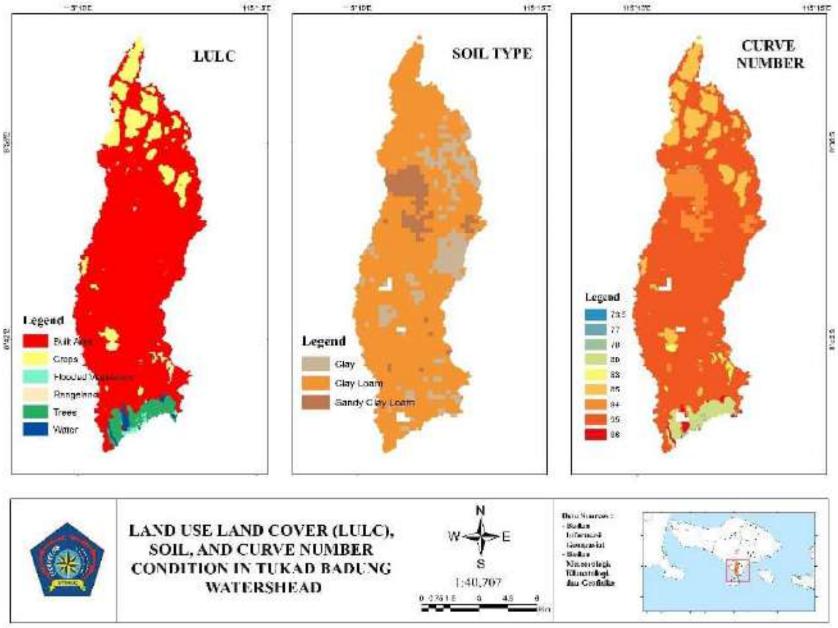

Figure 7. Land Use Land Cover, Soil Type, and Curve Number Mapping Condition in Tukad Badung Watershed

Land use and land cover in the Tukad Badung Watershed are divided into six classifications. Built-up Areas include developed land such as residential areas, highways, and urban infrastructure. Crops include agricultural land regularly cultivated for food crops such as corn, wheat, and soybeans. Flooded vegetation consists of vegetation inundated for most of the year, including mangroves, rice paddies, and flooded intensive agriculture. Rangeland includes shrubland and rocky wasteland or barren land without vegetation. Trees refer to vegetation with a minimum height of 15 meters found in dense forests, swamps, and mangroves. Water covers areas with a consistent presence of water such as rivers, lakes, reservoirs, and harbors (Yuan et al., 2025).

Based on Figure 7, the LULC classification in the Tukad Badung Watershed is dominated by built-up areas covering 68.86 km^2, or 83.09% of the total area. This dominance is closely linked to the watershed's geographical position, most of which lies within the City of Denpasar as the economic and tourism hub and capital of Bali Province, driving rapid growth in built-up land. Such extensive built-up areas tend to increase surface runoff due to limited infiltration (Laban et al., 2025). The second-largest LULC category is agricultural land, covering 9.14 km^2 or 11.03% of the watershed area, concentrated in the upstream section where higher elevations, fertile soil, and a cooler climate make it suitable for agriculture and plantations. These topographic characteristics help protect the upstream area from land-use conversion, unlike the downstream section, which tends toward urban development.

The downstream section otherwise consists of forested vegetation where the river discharges and connects directly to the ocean.

Soil types in the Tukad Badung Watershed consist primarily of clay loam, covering 65.28 km^2 or 79.64% of the area. The second most common type is clay, covering 11.10 km^2 or 13.54%, followed by sandy clay loam at 5.58 km^2 or 6.81%. Clay loam has a higher water-holding capacity than sandy textures, with a consistency that is somewhat slippery, sticky, and easily moldable (Mutmainnah et al., 2021). These properties influence the soil's ability to allow water to permeate into underlying layers. According to the Food and Agriculture Organization (FAO) (1990), clay loam soils have an infiltration capacity of 0.5 to 1.0 cm/hour, classified as low to moderate, meaning rainfall is not optimally absorbed and surface runoff volume potentially increases. This condition is further compounded by the high proportion of built-up areas in the watershed, which reduces infiltration and accelerates runoff concentration toward the river channel. The combination of clay-loam soil and dominant impervious land creates conditions prone to flooding, especially during heavy rainfall events.

Based on the combined land use, land cover, and soil type data, CN values in the Tukad Badung Watershed range from 73.5 to 98. The highest CN value dominating the area is 95, covering 62.95 km^2 or approximately 76.8% of the watershed, a dominance closely linked to extensive built-up areas on clay-loam soils that directly limit infiltration. In the upstream section, the CN value recorded is 85, covering 9.08 km^2 or 11.07% of the basin, reflecting continued agricultural dominance on relatively more permeable soil that allows more effective infiltration than the urban middle and downstream sections. In the downstream section, the CN value tends to be lower at 80, covering 2.82 km^2 or 3.45% of the watershed, likely due to tree vegetation around the estuary that helps slow surface runoff. A small area with a CN of 98, covering 0.54 km^2 or 0.65%, is concentrated at the river estuary and reflects nearly impermeable land conditions. CN itself is a key parameter for estimating surface runoff, where lower values indicate greater infiltration capacity and higher values indicate a greater proportion of rainfall becoming runoff (Ideawati et al., 2015; Tikno et al., 2012). With a CN distribution heavily dominated by high values, the Tukad Badung watershed has limited infiltration capacity and tends to produce significant runoff even during moderate rainfall events.

3. Analysis Flood Inundation Distribution

Based on an analysis of meteorological factors and land cover, as well as information reported by Balipost (2025), the flood peak occurred on September 10, 2025, at 5:00 a.m. WITA. When converted to Coordinated Universal Time (UTC), the flood peak occurred on September 9, 2025, at 21:00 UTC. The flood distribution is shown in Figure 8 below.

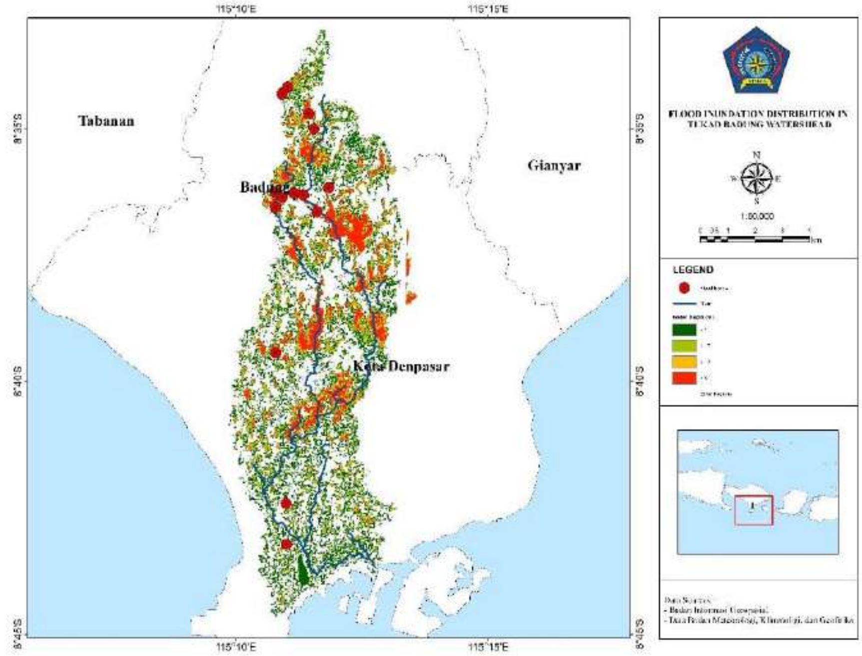

Figure 8. Flood Distribution Map for September 9, 2025, at 21:00 UTC

Flood depths exceeding 3 meters occur mainly in the upper watershed within Badung Regency and extend into the densely populated middle section of Denpasar City, where river overflow directly inundates residential and commercial areas. This severity stems from the conversion of natural land cover into built-up areas, which lowers infiltration capacity and concentrates runoff toward the channel, a mechanism consistent with the Gajahwong River in Yogyakarta, where built-up land covering 48% of the watershed similarly drove a high runoff coefficient and severe inundation (Sari et al., 2025). Built-up areas in Tukad Badung cover an even greater share of the watershed at 83.09%, which helps explain why flood depths here exceed those reported for less urbanized Indonesian catchments. Inundation depths of 2 to 3 meters occur fairly evenly along the main channel of the Tukad Badung River as it flows north to south, a pattern shaped by the channel's confinement within clay loam soils of low infiltration capacity that force excess rainfall to remain as surface flow. Depths of 1 to 2 meters extend more broadly on both sides of the main channel as tributary streams draining the surrounding built-up terrain add runoff beyond direct river overflow. This depth range is comparable to the Majalaya Watershed in Bandung, where similar upper catchment urbanization contributed to flood depths within the same range under comparable rainfall intensity (Rohmat et al., 2022).

In the downstream section bordering the southern coast of Denpasar City, flood depths remain below 1 meter despite continued flooding, since the limiting factor there is less land cover and more the estuary's low gradient and tidal backwater effect, which slows outflow rather than generating additional runoff. This contrast shows that flood severity in the Tukad Badung Watershed follows a downstream gradient, governed primarily by land use and slope upstream and by hydraulic and tidal constraints near the coast. These simulated depths are broadly consistent with earlier HEC-RAS studies of the Tukad Badung River, which found the channel could still accommodate design discharge at longer return intervals under earlier land cover conditions (Suryatmaja et al., 2024; Wiarta et al., 2008), with the deeper inundation identified here reflecting the intervening decades of built-up area expansion rather than a discrepancy in modeling approach. Part of the remaining difference may also stem from the use of SRTM 30 m as terrain input, since coarser resolution tends to smooth narrow channel geometry and embankment features that influence local inundation extent. This limitation is consistent with findings from the Katulampa Watershed, Indonesia, where SRTM underperformed the finer-resolution ALOS and even the coarser MERIT-Hydro dataset in reproducing observed flood hydrographs, indicating that DEM resolution alone does not guarantee modeling accuracy (Ginting et al., 2024). This interpretation is nonetheless reinforced by the spatial correspondence between observed and modeled flood locations across the watershed.

In addition to visual validation using maps, model validation was further supported by a statistical approach using the Hit Rate (HR) method, chosen because the available validation data consisted only of flood event locations without water depth information, requiring a binary evaluation of whether each location was captured within the model's flood distribution. The results of the calculations are shown in Table 2.

Table 2. Modelling Validation

Variable	Value
TP	10 Events
FN	2 Events
Hit Rate	83.33 %

Based on the table, the HEC-RAS model correctly predicted 10 of the 12 recorded flood locations (True Positives), yielding a Hit Rate of 83.33%, above the commonly used 75% threshold for acceptable model performance. The two missed locations (False Negatives) likely reflect the resolution limitation of the SRTM 30 m terrain input discussed earlier, as narrow drainage features smaller than the DEM's grid cell are unlikely to be captured in the simulated inundation extent. This indicates the model represents flood conditions well at the watershed scale, though less reliably for highly localized flooding, and can be considered suitable as a reference for spatial analysis of flood distribution in the Tukad Badung Watershed.

D. CONCLUSION AND SUGGESTION

This study yielded several conclusions. During the September 9 to 10, 2025 flood event in the Tukad Badung Watershed, meteorological parameters indicated abnormal conditions compared to typical patterns. Extreme rainfall was recorded at the Abiansemal Rain Gauge Station (ARG) and the Tuban Automatic Weather Station (AWS), reaching 284.6 mm and 116 mm respectively, while temperature, air pressure, wind speed, and evapotranspiration showed similarly anomalous conditions alongside a dominant northwest wind direction. Land cover in the Tukad Badung River Basin is dominated by settlements from upstream to downstream, a condition that further intensified the flooding. Flood inundation distribution was simulated using HEC-RAS software, and validation results indicate the model effectively represents actual flood conditions, evidenced by a Hit Rate of 83.33%.

This study has several limitations. First, the land cover and soil type data used do not fully reflect conditions at the time of the flood, so more up to date data is needed to improve simulation accuracy. Second, the SRTM 30 m terrain input limits detection of fine-scale drainage features, as noted in the Discussion. Third, there is a lack of flood location data with depth information, which limits the scope of model validation and may introduce bias into the accuracy evaluation. Despite these limitations, the findings offer practical value for policymakers responsible for flood-prone area management, as the flood distribution maps can serve as a reference for monitoring severely affected areas and supporting disaster mitigation planning. Future research should update the input data to reflect current land use and hydrological conditions, use finer resolution DEM sources such as DEMNAS or LiDAR, and prioritize collecting observed inundation depth data for validation, since this study relies on BNPB flood reference points rather than direct depth measurements.

ACKNOWLEDGMENTS

The author would like to express gratitude to the Indonesian Meteorology, Climatology, and Geophysics Agency (BMKG) and the State College of Meteorology, Climatology, and Geophysics (STMKG) for facilitating and fully supporting the entire research process, enabling it to be carried out successfully.

REFERENCES

Ahmad, D., & Afzal, M. (2022). Flood hazards and livelihood vulnerability of flood-prone farm-dependent Bait households in Punjab, Pakistan. *Environmental Science and Pollution Research*, *29*(8), 11553–11573. https://doi.org/10.21203/rs.3.rs-327153/v1

Anggreni, R., Muliadi, M., & Adriat, R. (2018). Analisis Pengaruh Tutupan Awan Terhadap Radiasi Matahari di Kota Pontianak. *PRISMA FISIKA*, *6*. https://doi.org/10.26418/pf.v6i3.28896

Aryastana, P. (2015). Identifikasi Pemanfaatan Daerah Sempadan Sungai Tukad Ayung. *PADURAKSA: Jurnal Teknik Sipil Universitas Warmadewa*, *4*(1), 17–25.

Asdak, C. (2010). Hydrology and watershed management. *Yogyakarta: Gadjah Mada University*.

Audah, S., Cahyadi, M. N., & Taufik, M. (2017). Analisa Penentuan Water Vapor Terhadap Pengaruh Erupsi Gunung Sinabung Menggunakan Data SUGAR Dan Citra Satelit Terra MODISs. *Jurnal Inotera*, *2*(1), 37.

Aulia, H., Kumalawati, R., Muhtar, G. A., & Ayuningtyas, E. A. (2023). Analisis Kerentanan Bencana Banjir dari Data Intesitas Hujan di Badung Provinsi Bali. *Jurnal Ilmiah Multidisiplin*, *2*(03), 17–20. https://doi.org/10.56127/jukim.v2i03.611

Bakar, A. (2024). Analysis of the Impact of the Flood Disaster on the Existence of Community Socio-Economic Life. *Jurnal Sosial Humaniora*, *15*(1), 71–87. https://doi.org/10.30997/jsh.v15i1.9859

Balipost. (2025). *Banjir 10 September Terjadi di 7 DAS*. 1 Oktober. https://www.balipost.com/news/2025/10/01/494129/Banjir-10-September-Terjadi-di...html

BBC. (2025). *Banjir Bali terparah sepanjang satu dekade, korban meninggal bertambah menjadi 16 orang*. 12 September. https://www.bbc.com/indonesia/articles/cj9z0m8zd9lo

BBMKG Wilayah III. (2025). *Buletin Informasi Cuaca, Iklim, dan Gempa Bumi Provinsi Bali* (Tahun XIX). BBMKG Wilayah III.

BMKG. (2023). *Standar Operasional Prosedur (SOP) tentang Penyediaan dan Penyebarluasan Peringatan Dini Cuaca Ekstrem Sesaat (Nowcasting) 1 (satu) sampai dengan 3 (Tiga) Jam ke Depan di Lingkungan Badan, Meteorologi, Klimatologi, dan Geofisika*.

BNPB. (2025). *Data Bencana Indonesia 2024* (Volume 3,). Pusat Data Informasi dan Komunikasi Kebencanaan Badan Nasional Penanggulangan Bencana. https://bnpb.go.id/storage/app/media/Buletin Info Bencana/Buku Data Bencana 2024/20250613_Buku Data 2024.pdf

Bragg, M. A., Poudel, A., & Vasconcelos, J. G. (2025). Comparing SWMM and HEC-RAS hydrological modeling performance in Semi-Urbanized watershed. *Water*, *17*(9), 1331.

Brunner, G. W. (2016). *HEC-RAS—River Analysis System. User's Manual. Version 5.0.* US Army Corps of Engineers, Hydrologic Engineering Center.

Danumah, J. H., Odai, S. N., Saley, B. M., Szarzynski, J., Thiel, M., Kwaku, A., Kouame, F. K., & Akpa, L. Y. (2016). Flood risk assessment and mapping in Abidjan district using multi-criteria analysis (AHP) model and geoinformation techniques, (cote d'ivoire). *Geoenvironmental Disasters*, *3*(1). https://doi.org/10.1186/s40677-016-0044-y

Davie, T. (2019). *Fundamentals of Hydrology*. Routledge.

Desalegn, H., & Mulu, A. (2021). Mapping flood inundation areas using GIS and HEC-RAS model at Fetam River, Upper Abbay Basin, Ethiopia. *Scientific African*, *12*, e00834.

Erwanto, Z., Nugroho, F. A., & Hardiyanti, S. A. (2021). Prediksi Iklim Berdasarkan Korelasi Evapotranspirasi Potensial Rata-Rata Tahunan Terhadap Curah Hujan Total Tahunan Di DAS Banyuwangi. *Pertemuan Ilmiah Tahunan HATHI ke-38. PIT HATHI*, 377–388.

FAO. (1990). *FAO Land and Water Development Division, Food and Agriculture Organisation of the United Nation*.

Ginting, B., Lidyana, P., Christopher, C., Yudianto, D., & Yuebo, X. (2024). Evaluating the satellite-derived DEM accuracy with rain-on-grid modeling for flood hydrograph prediction of Katulampa Watershed, Indonesia. *International Journal of River Basin Management*, *23*, 369–386. https://doi.org/10.1080/15715124.2024.2312857

Ideawati, L. F., Limantara, L. M., & Andawayanti, U. (2015). Analisis perubahan bilangan kurva aliran permukaan (runoff curve number) terhadap debit banjir di das lesti. *Jurnal Teknik Pengairan*, *6*(1), 37–45.

Iswardoyo, J., & Satria, H. (2023). Analisis Daerah Terdampak Banjir Bandang Menggunakan HEC-RAS 2 Dimensi di Sungai Sat, Kabupaten Pati, Jawa Tengah. *Jurnal Teknik Hidraulik*, *14*(1), 13–26. https://doi.org/10.32679/jth.v14i1.717

Jabbar, A., Putri, I., & Herol, H. (2023). Analisis Potensial Pengaruh Perubahan Tata Guna Lahan dan Iklim Terhadap Sumber Daya Air DAS Bekasi dengan Menggunakan Model Hidrologi. *JURNAL TEKNIK SIPIL*, *4*, 6–12. https://doi.org/10.37366/jts.v4i2.3942

Laban, S., Zubair, H., Nugraha, F., & Fajeriana, N. (2025). Pemodelan Hidrograf untuk Menilai Pengaruh Perubahan Penggunaan Lahan Terhadap Karakteristik Aliran Sungai Di Sub-DAS Tanralili, Sulawesi Selatan. *Jurnal Penelitian Pengelolaan Daerah Aliran Sungai*, *9*, 1–22. https://doi.org/10.59465/jppdas.2025.9.1.1-22

Lavers, D. A., Simmons, A., Vamborg, F., & Rodwell, M. J. (2022). An evaluation of ERA5 precipitation for climate monitoring. *Quarterly Journal of the Royal Meteorological Society*, *148*(748), 3152–3165. https://doi.org/10.1002/qj.4351

Mulyana, E. (2014). Pengaruh Angin Terhadap Pertumbuhan Awan Hujan di DAS Waduk PLTA Kota Panjang. *Jurnal Sains & Teknologi Modifikasi Cuaca*, *15*, 81. https://doi.org/10.29122/jstmc.v15i2.2674

Mutmainnah, D., Ayu, I. W., & Oklima, A. M. (2021). Analisis tanah untuk indikator tingkat ketersediaan lengas tanah di lahan kering kecamatan empang. *Jurnal Agroteknologi*, *1*(1), 27–38.

Patra, A., Oueslati, B., Chevallier, T., Renaud, P., Kervella, Y., & Dubus, L. (2025). Evaluation of ERA5, COSMO-REA6 and CERRA in simulating wind speed along the French coastline for wind energy applications. *Advances in Science and Research*, *22*, 69–85. https://doi.org/10.5194/asr-22-69-2025

Peker, İ. B., Gülbaz, S., Demir, V., Orhan, O., & Beden, N. (2024). Integration of HEC-RAS and HEC-HMS with GIS in flood modeling and flood hazard mapping. *Sustainability*, *16*(3), 1226. https://doi.org/10.3390/su16031226

Qian, J.-H. (2008). Why precipitation is mostly concentrated over islands in the Maritime Continent. *Journal of the Atmospheric Sciences*, *65*(4), 1428–1441. https://doi.org/10.1175/2007JAS2422.1

Rohmat, F. I. W., Sa'adi, Z., Stamataki, I., Kuntoro, A. A., Farid, M., & Suwarman, R. (2022). Flood modeling and baseline study in urban and high population environment: A case study of Majalaya, Indonesia. *Urban Climate*, *46*, 101332. https://doi.org/https://doi.org/10.1016/j.uclim.2022.101332

Sari, S. P., Suprayogi, S., & Budiman, S. (2025). HEC-RAS-based urban flood simulation for enhancing mitigation scenarios in the Gajahwong River, Indonesia. *Geographia Technica*, *20*(1), 127. https://doi.org/10.21163/GT_2025.201.10

Sarifah, F., Arashi, F. B., Iskandar, A. L., Ramadhan, M. A. R., Daniswara, M. P., & Rahmadhani, F. (2024). Analisis Dampak Bencana Banjir terhadap Kondisi Sosial dan Ekonomi pada Masyarakat. *BANDAR: Journal Of Civil Engineering*, *6*(2), 56–64.

Scharffenberg, W. A., & Fleming, M. J. (2006). *Hydrologic Modeling System HEC-HMS: User's Manual*. US Army Corps of Engineers, Hydrologic Engineering Center.

Selçuk, L., Selçuk, A., & Kasapoğlu, D. (2016). Urban flood susceptibility assessment of central districts of Van province, Turkey, using geographic information system (GIS)-based multi criteria decision analysis (MCDA) Coğrafi bilgi sistemleri (CBS) tabanlı çok kriterli karar analizi (Çkka) kullanılar. *Yerbilimleri/Earth Sciences*, *37*(1).

Setiawan, A., Tuna, M. S., Qulu, A. R., & Nugraheni, I. R. (2022). Analisis Secara Fisis Dan Dinamis Kejadian Hujan Penyebab Banjir di Makassar Tanggal 20 Februari 2022. *Jurnal Material dan Energi Indonesia*, *12*(01), 18–25.

Seto, T. (2011). Distribusi Temporal dan Spasial Tekanan Udara Terkait Pertumbuhan Awan di DAS Larona, Sulawesi Selatan. *Jurnal Sains & Teknologi Modifikasi Cuaca*, *12*, 55. https://doi.org/10.29122/jstmc.v12i2.2191

Shi, P., Lyu, K., Zhenya, L., Yang, T., Xu, C.-Y., Hao, X., & Xiao, J. (2025). A Novel Topography-Based Approach for Real-Time Flood Inundation Mapping. *Water Resources Research*, *61*. https://doi.org/10.1029/2024WR037851

Singer, M. B., Asfaw, D. T., Rosolem, R., Cuthbert, M. O., Miralles, D. G., MacLeod, D., Quichimbo, E. A., & Michaelides, K. (2021). Hourly potential evapotranspiration at 0.1° resolution for the global land surface from 1981-present. *Scientific Data*, *8*(1), 224. https://doi.org/10.1038/s41597-021-01003-9

Sulistya, W. (2022). Belajar dari kejadian bencana alam sepanjang tahun 2021. *Jurnal Widya Climago*, *4*(2), 84–90.

Suryadi, R., Putranto, D. D. A., & Juliana, I. C. (2022). Analisis 1D–2D Genangan Banjir pada Kawasan Perumahan Baturaja Permai, Kecamatan Baturaja Timur. *Cantilever: Jurnal Penelitian dan Kajian Bidang Teknik Sipil*, *11*(1), 39–48. https://doi.org/10.35139/cantilever.v11i1.115

Suryatmaja, I. B., Wangsa, A. A. R. R., Kurniari, K., & Prasetia, I. P. (2024). Pemodelan Kapasitas Air Pada Saluran Drainase dengan Program HEC-RAS (Studi Kasus: Jalan Cekomaria dan Jalan Padma Denpasar Timur). *Jurnal Ilmiah Kurva Teknik*, *13*(2), 127–136.

Swaminathan, S., & Tantri, B. R. (2024). Confusion Matrix-Based Performance Evaluation Metrics. *African Journal of Biomedical Research*, *27*, 4023–4031. https://doi.org/10.53555/AJBR.v27i4S.4345

Tikno, S., Hariyanto, T., Anwar, N., Karsidi, A., & Aldrian, E. (2012). Aplikasi metode Curve Number untuk mempresentasikan hubungan curah hujan dan aliran permukaan di DAS Ciliwung Hulu–Jawa Barat. *Jurnal Teknologi Lingkungan*, *13*(1), 25–36. https://doi.org/10.29122/jtl.v13i1.1402

Wasko, C., Nathan, R., Stein, L., & O'Shea, D. (2021). Evidence of shorter more extreme rainfalls and increased flood variability under climate change. *Journal of Hydrology*, *603*, 126994. https://doi.org/https://doi.org/10.1016/j.jhydrol.2021.126994

Wiarta, I. N., Yulistiyanto, B., & Nizam, N. (2008). Analisis Hidraulika Banjir Tukad Badung.

Civil Engineering Forum Teknik Sipil, *18*(2), 851–858.

Wijayanto, M. R., & Helda, N. (2022). Aplikasi Program HEC-RAS 5.0. 7 untuk Pemodelan Banjir di Sub-sub DAS Martapura Kabupaten Banjar. *Serambi Engineering*, *7*(4), 3868–3880. https://doi.org/10.32672/jse.v7i4.4799

Yuan, M., He, G., Wang, G., Yin, R., Zhang, Z., Long, T., & Peng, Y. (2025). Spatial Consistency and Accuracy Assessment of Grassland Classification in the Sanjiangyuan Region: From Six Medium Resolution Land Cover Products. In *Remote Sensing* (Vol. 17, Nomor 24, hal. 3983). https://doi.org/10.3390/rs17243983

Zhang, H., & Wang, L. (2021). Analysis of the variation in potential evapotranspiration and surface wet conditions in the Hancang River Basin, China. *Scientific Reports*, *11*(1), 8607. https://doi.org/10.1038/s41598-021-88162-2